PLoS one

Pre & Postsynaptic Tuning of Action Potential Timing by Spontaneous GABAergic Activity

Olivier Caillard[1,2]*

1 INSERM UMR641, IFR Jean-Roche, Marseille, France, 2 Université de la Méditerranée, Marseille, France

Abstract

Frequency and timing of action potential discharge are key elements for coding and transfer of information between neurons. The nature and location of the synaptic contacts, the biophysical parameters of the receptor-operated channels and their kinetics of activation are major determinants of the firing behaviour of each individual neuron. Ultimately the intrinsic excitability of each neuron determines the input-output function. Here we evaluate the influence of spontaneous GABAergic synaptic activity on the timing of action potentials in Layer 2/3 pyramidal neurones in acute brain slices from the somatosensory cortex of young rats. Somatic dynamic current injection to mimic synaptic input events was employed, together with a simple computational model that reproduce subthreshold membrane properties. Besides the well-documented control of neuronal excitability, spontaneous background GABAergic activity has a major detrimental effect on spike timing. In fact, $GABA_A$ receptors tune the relationship between the excitability and fidelity of pyramidal neurons via a postsynaptic (the reversal potential for $GABA_A$ activity) and a presynaptic (the frequency of spontaneous activity) mechanism. GABAergic activity can decrease or increase the excitability of pyramidal neurones, depending on the difference between the reversal potential for $GABA_A$ receptors and the threshold for action potential. In contrast, spike time jitter can only be increased proportionally to the difference between these two membrane potentials. Changes in excitability by background GABAergic activity can therefore only be associated with deterioration of the reliability of spike timing.

Introduction

Variability in neural activity is apparent throughout the central nervous system, in a wide range of electrophysiological signals. Several well recognized sources of noise in cortical neurons contribute to spike train variability, like the probabilistic release of transmitter and the stochastic gating of ion channels [1,2]. Evoked activities in stimuli-driven experiments are always superimposed on ongoing background activity, fluctuations of which contribute to the *in vivo* trial-to-trial variability [3–6]. Ongoing subthreshold activity of neocortical neurones is characterised by alternating states of low or intense synaptic activity [7,8], supported at least in part by two major neurotransmitters, GABA and glutamate. GABA activates mainly $GABA_A$ receptors, which first reduce the excitability of the cells by reducing the membrane resistance and second, according to their reversal potential, will bring the membrane potential away or close to the threshold for action potentials [9–11].

Two main functional roles have been established for spontaneous GABAergic activity. The first relates to the membrane time constant of the cell: if the passive properties of the cell are comparable to a resistor-capacitor circuit, with a capacitance proportional to the surface of plasma membrane, and a resistance inversely proportional to the number of open ion channels, strong activation of $GABA_A$ receptors leads to a decrease in the membrane time constant, which in turn speeds up dV/dt. As a consequence, individual excitatory postsynaptic currents are better resolved in time, and voltage changes are steeper [8,12,13]. The second is attributed to the background noise that creates a dynamic range in the input/output function of a neuron: referred to as stochastic resonance [14,15]: the processing of synaptic events by background activity, according to noise level or variability, translates the information provided by excitatory events into firing probability, despite the fact that this process is nonlinear [15–17]. Nevertheless, compelling evidence supports the fact that, even in individual cells, not only the average frequency of firing but also the timing of each action potential is relevant for neuronal information coding. Reliability in spike timing is known to be dependent on the structure of the excitatory stimulus [18]. The sequential activation of excitatory and inhibitory inputs in feed-forward networks [19] and the presence of functional GABAergic autapses at some fast-spiking interneurones [20] were shown to be relevant physiological mechanisms that can reinforce spike timing in neuronal networks. In spite of that, since most of the synaptic activity received either *in vitro* or *in vivo* appears to be uncorrelated to any specific stimulus, a yet unsolved question is what influence spontaneous GABAergic activity has on the temporal fidelity of pyramidal cell firing, according to the mode of activation of $GABA_A$ receptors [21] or their reversal potential [22].

Here we evaluate and quantify how spontaneous activation of $GABA_A$ receptors affects action potential firing and timing, according to the frequency of action potential discharge, and various modes of GABA release. We also evaluate the relative contribution of shunting inhibition and driving force for $GABA_A$ receptors to neuronal discharge.

Results

Spontaneous GABAergic activity tunes the temporal fidelity of Pyramidal Cell discharge

In order to evaluate the impact of spontaneous GABAergic activity received by L2/3 pyramidal neurones on their spike timing, gramicidin-perforated patch-clamp recordings Fig. 1). Although several precautions were taken, the possibility of an intermediated perforated-patch/whole-cell configuration cannot be completely excluded (see methods). Excitability, defined as the average firing rate, and fidelity measured as the average coefficient of variation of inter-spike intervals along the discharge (CV_{ISI}, see methods) were calculated for various DC steps. The influence of GABAergic activity on these parameters was tested by application of picrotoxin (PTX, 100 μM) a $GABA_A$ receptor blocker. Blockage of $GABA_A$ receptors, whilst not affecting resting Vm (average change -0.2 ± 0.9 mV, n = 7, P = 0.86) increased the excitability, reflected by a leftward shift of the frequency vs current relationship of recorded cells. Although CV_{ISI} was dependent on firing frequency in both control conditions and when $GABA_A$ receptors were blocked, the CV_{ISI} was reduced at comparable firing rates in the presence of PTX, especially for low rates of AP firing. When changes in excitability were normalised for each
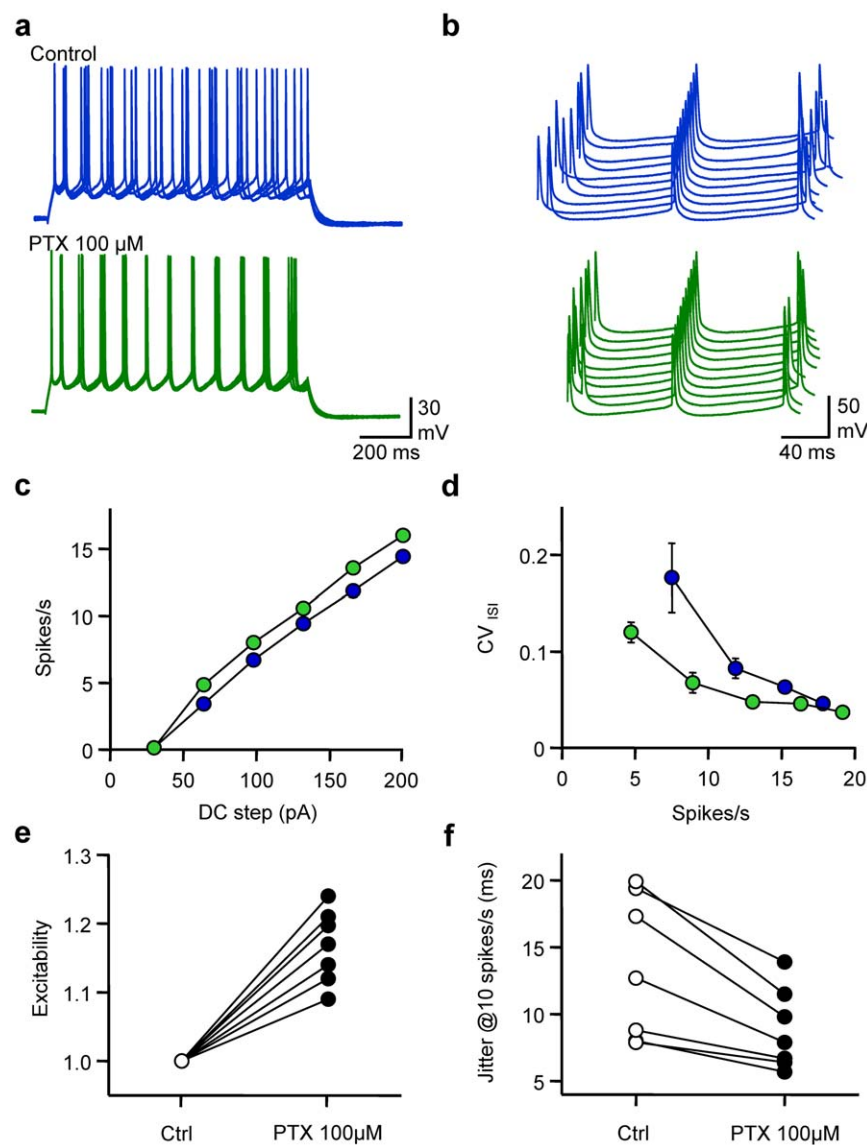
Figure 1. Spontaneous GABAergic activity affects excitability and spike timing of pyramidal cells. a, Superimposed (5) membrane potential (Vm) fluctuations of a gramicidin-perforated current-clamped L2/3 pyramidal cell in response to a DC step (1 s, 170 pA) before (control, blue) and after extracellular application of picrotoxin (100 μM, PTX, green). The cell was held at around -80 mV in both conditions. Same cell and colour code for b, c and d. b, Waterfall view of Vm when the 5th spike was set as the time reference. c, Mean firing rate vs DC step. d, Coefficient of Variation of the Inter Spike Interval (CV_{ISI}) vs firing rate. e, Normalised changes in excitability observed when adding PTX (n = 7). f, Changes in spike jitter for an interpolated firing rate of 10 spikes/s.
doi:10.1371/journal.pone.0022322.g001

individual cell as the average change in spike number at each DC step, a significant increase in intrinsic excitability was observed ($117\pm5\%$, n = 7, P<0.001). Spike time jitter, defined as the standard deviation of the average ISI, was calculated when interpolating CV_{ISI} at a firing rate of 10 spikes/s. While spike time jitter was quite heterogeneous from one cell to another in control conditions (range 6.6–19.9 ms), it was always reduced after PTX application. On average, blocking $GABA_A$ receptors significantly reduced spike time jitter from 13.4 ± 5.4 ms to 8.8 ± 3.0 ms ($68\pm10\%$, n = 7, P<0.05). Thus, GABAergic activity controls both excitability and fidelity of pyramidal cell discharge.

Presynaptic control of temporal fidelity

In order to quantify the contribution of various levels of GABAergic activity to pyramidal cell discharge parameters, currents mimicking spontaneous GABAergic events were injected in whole-cell recorded neurones by means of a dynamic-clamp amplifier in the presence of PTX (100 µM). Patterns of spontaneous GABAergic synaptic conductances were constructed by convoluting the occurrence in time of unitary events with a conductance transient template that had similar characteristics to the average event measured experimentally (Fig. S1). The time of occurrence of each event obeyed a Poisson law and was determined extemporaneously according to the desired target rate of spontaneous activity. In a first set of experiments the reversal potential for $GABA_A$ receptors (E_{GABA}) was set at -70 mV (Fig. 2). Experiments were performed at rates of GABAergic events going from 0 (control conditions) to 100 events/s. Both excitability and fidelity varied according to the level of $GABA_A$ activity. When changes in excitability were normalised for each recorded neuron, 3-10-33-100 events/s reduced excitability by $0.3\pm1\%$ (n = 7, P = 0.085), $8\pm2\%$ (n = 9, P<0.001), $15\pm1\%$ (n = 14, P<0.0001) and $44\pm3\%$ (n = 12, P<0.0001) respectively. When spike time jitter at a firing rate of 10 spike/s was normalised in the absence of GABAergic activity for each recorded cell, 3-10-33-100 events/s increased spike time jitter by $148\pm14\%$ (n = 7, P<0.05), $157\pm15\%$ (n = 9, P<0.005), $209\pm20\%$ (n = 17, P<0.0001), $316\pm32\%$ (n = 15, P<0.0001) respectively. Thus, spontaneous $GABA_A$ activity not only reduces neuronal excitability, but has a far more significant effect in deteriorating spike time precision.

Fidelity, not excitability depends on the mode of $GABA_A$ activation

In order to verify the conclusions drawn from the experimental data and further analyse the correlation between the rate of the spontaneous activity input, the output firing rate and the fidelity of neuronal discharge, we used a "leaky integrate and fire" with Random action potential Threshold (RT-LIF) model [23,24], in order to focus upon the subthreshold membrane properties according to $GABA_A$ activation while excluding the mechanisms responsible for action potential triggering. The standard deviation of the threshold was set to 1 mV so that frequency-dependent jittering resembling the experimental data was observed. The model consistently reproduced the firing behaviour of L2/3 pyramidal cells with realistic membrane time constant in the absence of synaptic activity (Fig. S2). Both excitability and fidelity were affected proportionally to the level of $GABA_A$ activity (Fig. 3). As for dynamic-clamp in vitro experiments, spike time jitter evaluated from RT-LIF was much more prone to changes, according to $GABA_A$ activity and firing rate. Thus for a rate of 10 spikes/s, 8 $GABA_A$ events/s were sufficient to increase jitter by 50%, while reducing excitability by only 2%. Both the transient changes in current and membrane resistance associated with $GABA_A$ activity contributed to these effects (Fig. S3) and when one

or the other constituent was annulled, the impact of changes in $GABA_A$ activity on excitability and fidelity was reduced. The charge of the random $GABA_A$ conductance transients determined the impact of random $GABA_A$ activity on both excitability and spike timing. Indeed, the detrimental effects of $GABA_A$ activity were proportional to the peak $GABA_A$ conductance (Fig. S4), while for a fixed $GABA_A$ charge, slowing or speeding up $GABA_A$ conductance transient kinetics did not affect the impact of $GABA_A$ activity on neither excitability or spike timing (Fig. S5).

The influence of the waveform pattern of $GABA_A$ activity was then tested on the number and precision of spikes emitted during the injection of various DC steps: the first mimicked the experimental spontaneous activity received by pyramidal neurones in vitro (Fig. S1); the second mode corresponded to an invariable pattern of $GABA_A$ conductance transients but consistently replayed, so that these G_{GABA-A} transients were time-locked during the different simulations; the third mode corresponded to a constant G_{GABA-A}, i.e. tonic activity [21], which was an average over time of the conductance transients received by the RT-LIF in the previous two modes.

When compared to control conditions, i.e. no GABAergic activity, a rate of 33 randomly occurring G_{GABA-A} transients per second notably increased spike time jitter, and both excitability and the fidelity of discharge were reduced (Fig. 4). When $GABA_A$ conductance transients were evoked invariably in time, despite the fact that the excitability was modified to the same extent as with random input, spike time jitter was much less affected. Although CV_{ISI} was larger than in control conditions, especially at low firing rates, it was smaller than the conditions in which randomly occurring spontaneous activity was generated. Last, the impact of a constant activation of $GABA_A$ conductance was tested (i.e. tonic activation of $GABA_A$ receptors [21]). Again, the decrement in excitability was comparable to other modes of $GABA_A$ activation, but CV_{ISI} vs firing rate relationship was close to control conditions. In order to get a comprehensive view of the impact of the different modes of $GABA_A$ activation, FI curves were drawn for a range of 0 to 100 events/s in the 3 modes defined above. While FI curves were comparably shifted to the right by $GABA_A$ activity in a frequency dependent manner, whatever the mode, the effect of $GABA_A$ activity on CV_{ISI} was highly dependent on the mode. In fact, spike-timing fidelity was noticeably reduced only if the cell, firing at low rate, received a high level of random $GABA_A$ activity.

In order to confirm that $GABA_A$ activation modes can affect spike timing in a different ways, an alternative type of spike timing analysis was performed (Fig. 5). Thus, instead of analysing the variability of the ISI along the discharge, the timing of action potentials initiated over 50 presentations was measured in control conditions and in the 3 different modes of $GABA_A$ activation. The DC step was adjusted in order to get an average rate of 5 spikes/s in all 4 conditions. Once each AP was detected, the timing data was convolved with a Gaussian waveform, in order to reflect both reliability and temporal precision of spike initiation. In control conditions, temporal organisation faded with time, but was still relatively high at the end of the discharge. In contrast, random patterns (33 events/s) of GABAergic activity rapidly disrupted the temporal organisation of the discharge. When the pattern of GABAergic activity was invariably replayed, peaks of AP initiation probability were higher in number than in control conditions, and varied in amplitude and width such that for specific time intervals AP initiation probability was higher than in control conditions. Last, in the presence of tonic activity, temporal dispersion and variance waveform were close to control conditions until the last third of the discharge.
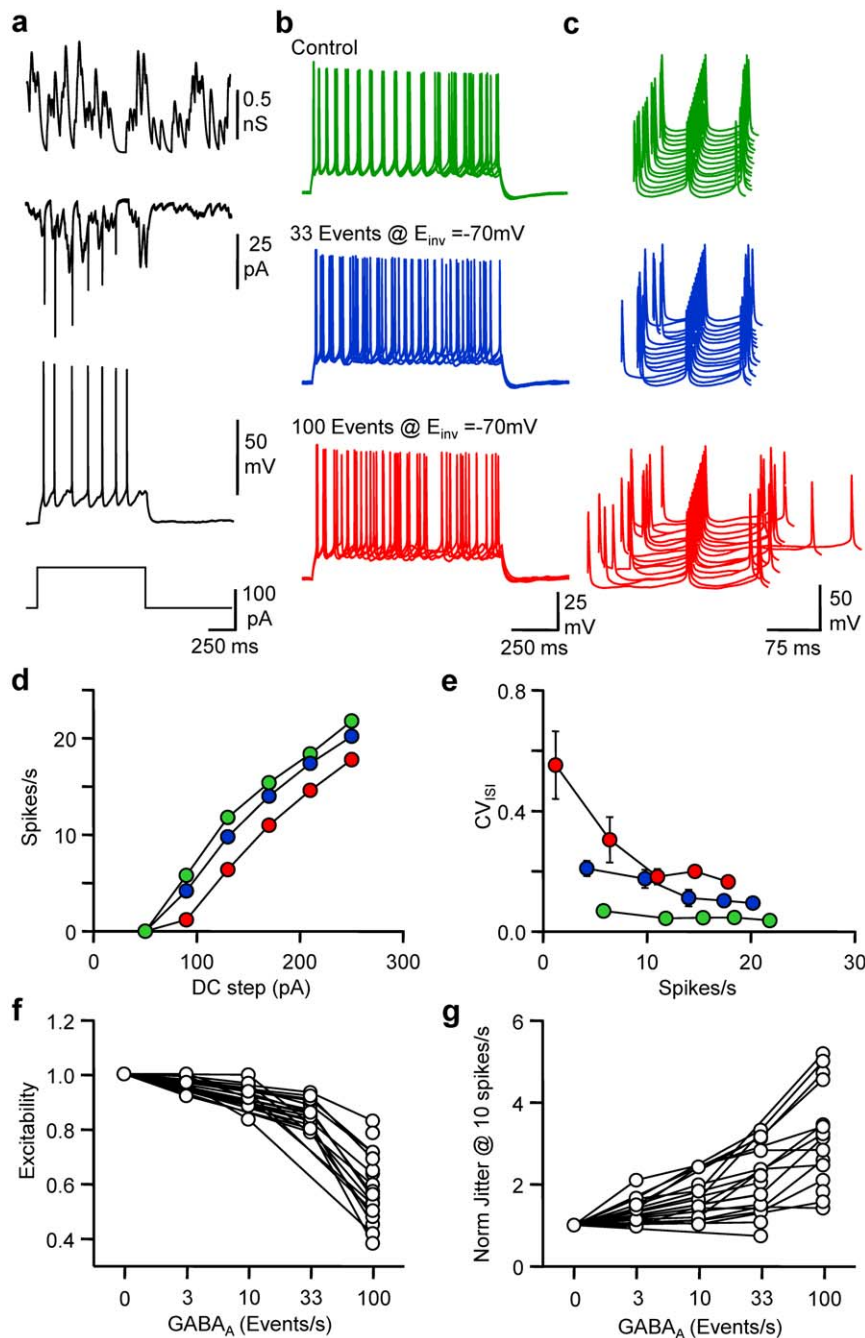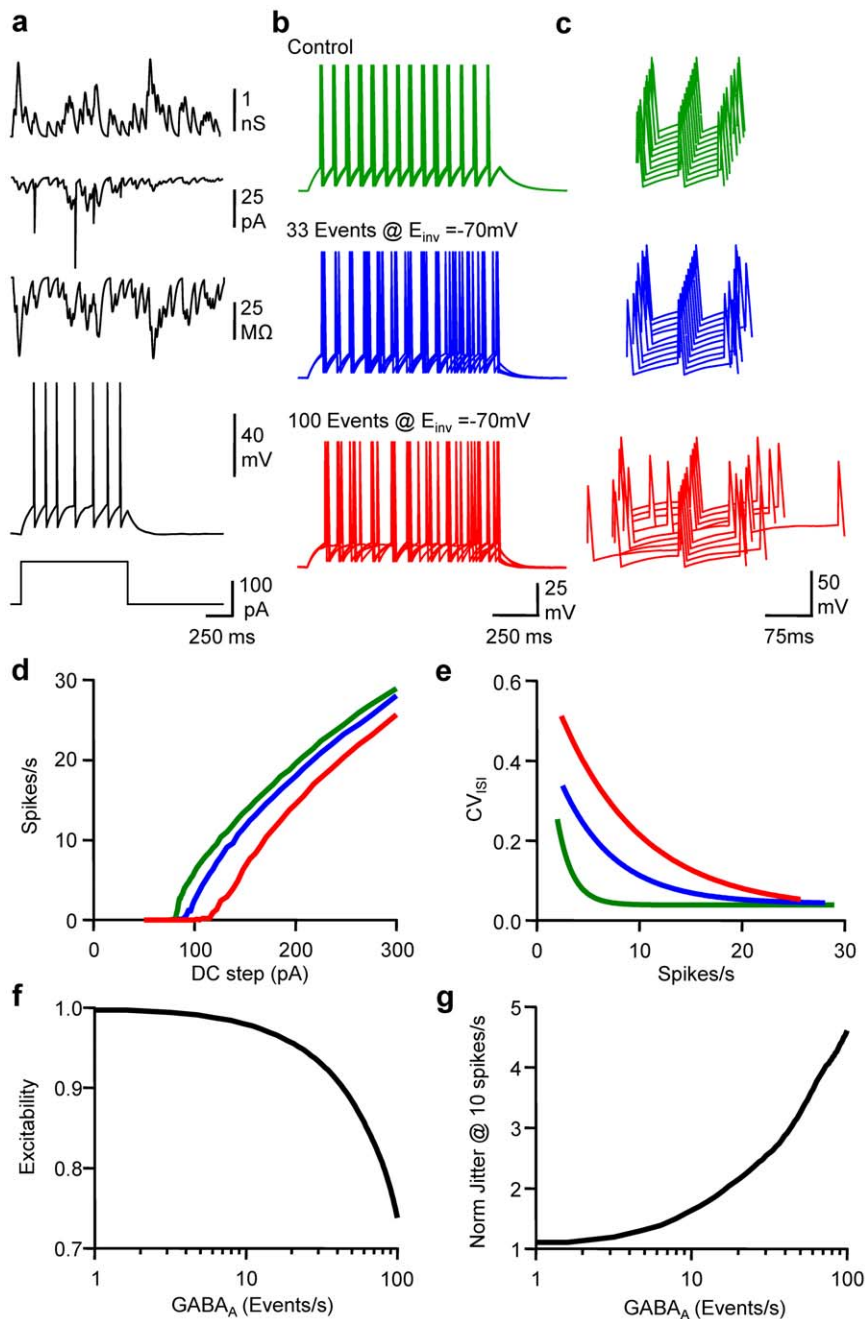
Figure 2. Frequency-dependent tuning of pyramidal cell excitability and spike timing. a, From upper to lower, an example of a $GABA_A$ conductance (G_{GABA-A}) pattern of 33 events/s, $GABA_A$ current (I_{GABA-A}), Vm and the DC protocol in a dynamic clamp recording of a L2/3 pyramidal cell. b, Superimposed (5) Vm fluctuations in response to a DC step (1 s, 170 pA) in control (green), in the presence of 33 (blue) or 100 (red) randomly occurring $GABA_A$ events/s dynamically injected with E_{GABA} set at -70 mV. Same cell and colour code for c,d and e. c, Waterfall view of Vm when the 5th spike was set as the time reference. d, Mean Firing rate *vs* DC step. e, CV_{ISI} *vs* mean spike firing rate. f, Normalised changes in excitability observed when neurons receive different levels of randomly occurring $GABA_A$ events/s. g, Normalised changes in spike jitter for an interpolated firing rate of 10 spikes/s.
doi:10.1371/journal.pone.0022322.g002

Thus, in contrast to invariable phasic or tonic $GABA_A$ activity, randomly occurring spontaneous $GABA_A$ activity has a major detrimental effect on spike timing.

Postsynaptic control of spike timing fidelity

In order to test the influence of E_{GABA} on excitability and fidelity, dynamic currents mimicking spontaneous GABAergic events were injected in pyramidal neurones at an average rate of

33 events/s in the presence of PTX (100 µM). The effects of spontaneous $GABA_A$ transients were first compared for $E_{GABA} = -70$ mV and -30 mV (Fig. 6). While a decrease in excitability and an increase in spike jitter was observed for $E_{GABA} = -70$ mV, a slight increase in excitability was noted for $E_{GABA} = -30$ mV, while the spike jitter was similar to control conditions. Quantification of changes in excitability at various firing rates showed that the FI curve was shifted either leftward or
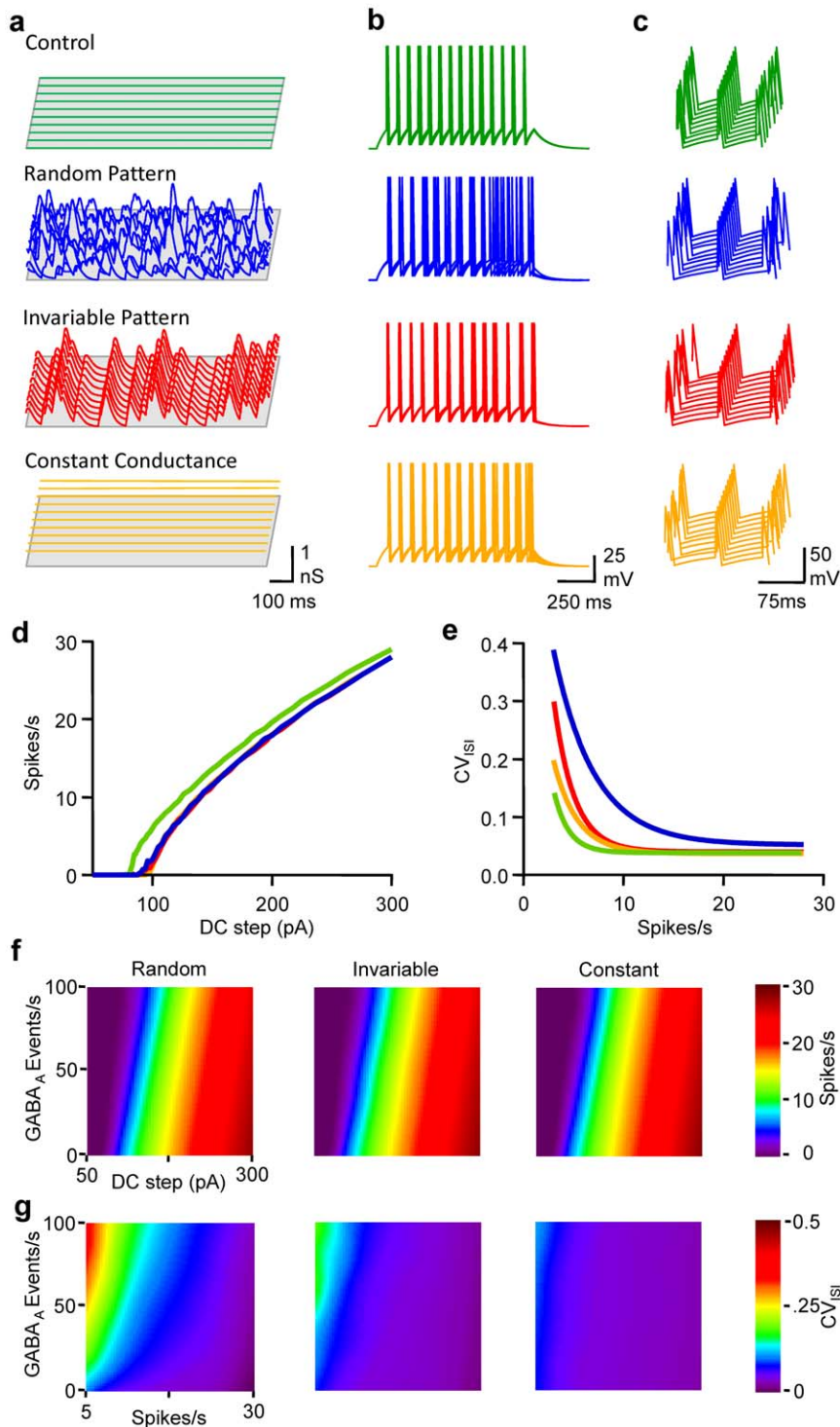
Figure 3. Modelling frequency-dependent tuning of neuronal excitability and spike timing. a, From upper to lower, an example of G_{GABA-A} pattern of 33 events/s, I_{GABA-A}, R_{in}, Vm and a DC step (1 s, 120 pA) when running the LIF model. b, Superimposed (5) Vm fluctuations in response to a DC step (1 s, 160 pA) in control (green), in the presence of 33 (blue) or 100 (red) randomly occurring $GABA_A$ events/s with E_{GABA} set at −70 mV. Same cell and colour code for c,d and e. c, Waterfall view of Vm when the 5th spike was set as time reference. d, Mean Firing rate *vs* DC step. e, CV_{ISI} *vs* firing rate. f, Normalised changes in excitability observed when LIF received 1 to 100 randomly occurring $GABA_A$ events/s. g, Normalised changes in spike jitter for a firing rate of 10 spikes/s.
doi:10.1371/journal.pone.0022322.g003

rightward according to E_{GABA}. While major changes in CV_{ISI} were observed for all firing rates tested at $E_{GABA} = −70$ mV, they were negligible at $E_{GABA} = −30$ mV. A series of experiments were performed with a broad range of E_{GABA} (from −80 to 0 mV) in order to establish the relationship between E_{GABA}, excitability and fidelity. Pyramidal neurone excitability was linearly dependent on E_{GABA} and changes in excitability were abolished when E_{GABA} was 6.1 mV under the AP threshold (n = 9; 95% confidence interval 10.3/1.9 mV under AP threshold). The relationship

between normalised jitter for an interpolated firing rate of 10 spikes/s was bell-shaped, with a minimum of 1.33 (n = 9; 95% confidence interval 1.12/1.54) for E_{GABA} being 2.5 mV under the AP threshold.

On/Off Control in Spike Timing tuning by $GABA_A$ reversal potential

To further analyze the relationship between the reversal potential for $GABA_A$ receptors, the rate of firing and spike timing, an initial

Figure 4. Randomly occurring GABA$_A$ conductance transients underlie the frequency-dependent tuning of pyramidal cell discharge fidelity. a, Waterfall view of conductance fluctuations injected into the LIF model in control conditions (no conductance, green), when the LIF model received 33 randomly occurring GABA$_A$ events/s (blue), an invariable pattern of 33 GABA$_A$ events/s (red), or when the neuron model received a constant G$_{GABA-A}$ equivalent to the average conductance for a rate of 33 events/s (orange). Same cell and colour code for b,c,d and e. b, Superimposed (5) Vm fluctuations of the LIF model in response to a DC step (1 s, 160 pA) in the various conditions depicted in a. c, Waterfall view of Vm when the 5th spike was set as the time reference. d, Mean firing rate *vs* DC step. e CV$_{ISI}$ *vs* firing rate. f, Mean firing rate displayed on a pseudocolor scale *vs* DC step and rate of GABA$_A$ activity when LIF model received random (left), invariable (middle) or constant conductance (right). g, CV$_{ISI}$ displayed on a pseudocolor scale *vs* firing and GABA$_A$ activity rate. Same conditions as in f.
doi:10.1371/journal.pone.0022322.g004
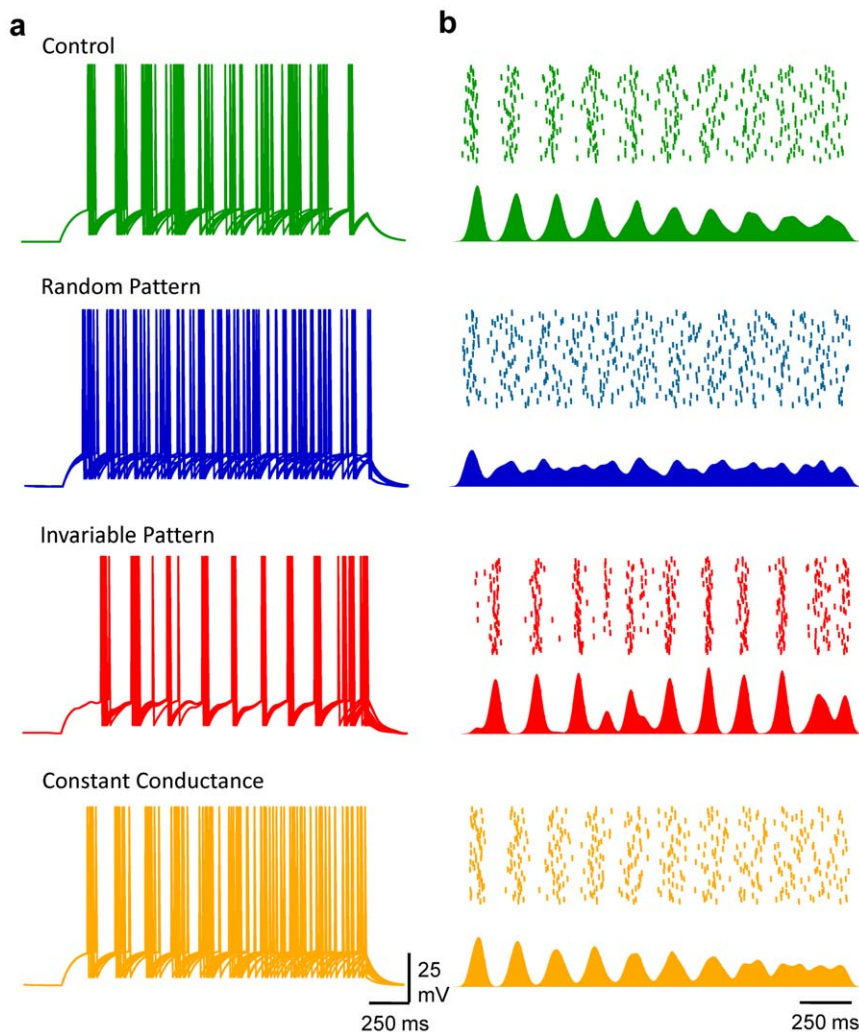
Figure 5. Randomly occurring GABA$_A$ conductance transients underlie the frequency-dependent tuning of pyramidal cell discharge fidelity. a, Superimposed (10) Vm fluctuations of the LIF model in response to a DC step (2 s) that allows a firing rate of 5 spikes/s, in control conditions (green, 95 pA), when the LIF model received 33 randomly occurring GABA$_A$ events/s (blue, 111 pA), an invariable pattern of 33 GABA$_A$ events/s (red, 110 pA), or when the neuron model received a constant G$_{GABA-A}$ equivalent to the average conductance for a rate of 33 events/s (orange, 110 pA). b up, Raster plot of spike times collected from 50 consecutive trials in the various conditions depicted in a; down, Spike probability over time for these 50 consecutive trials.
doi:10.1371/journal.pone.0022322.g005

simulation was performed with RT-LIF receiving an input rate of 33 random GABA$_A$ conductance transients per second. E$_{GABA}$ and DC steps varied from −90 to 0 mV and 50 to 300 pA, respectively (Fig. 7). While an increase in spike jitter, associated with an increase in interspike interval was obvious for E$_{GABA}$ = −70 mV, it was similar to control conditions for E$_{GABA}$ = −35 mV. Both transient changes in current and membrane resistance led to changes in excitability and fidelity (Fig. 7). Modifications in excitability were abolished when E$_{GABA}$ was 5 mV above AP threshold. When considering spike timing, a bell-shaped relationship between CV$_{ISI}$ and E$_{GABA}$ was observed with a minimum at 10 mV above AP threshold. When transient changes in membrane resistance were annulled, changes in excitability were abolished if E$_{GABA}$ was 10 mV under AP threshold and the CV$_{ISI}$ was minimal when E$_{GABA}$ was 5 mV under AP threshold. Thus GABA$_A$ currents can almost compensate for the decrease in the fidelity of spike timing and excitability induced by the reduction in membrane resistance when E$_{GABA}$ is slightly above the AP threshold.

In order to get a better view of the impact of spontaneous GABA$_A$ activity on excitability and spike time jitter at different E$_{GABA}$, FI curves were drawn for a range of 0 to 100 events/s at 3 different E$_{GABA}$. FI curves were shifted right and left by GABA$_A$ activity in a frequency dependent manner for E$_{GABA}$ = −70 mV and E$_{GABA}$ = 0 mV respectively. However at E$_{GABA}$ = −35 mV increasing GABA$_A$ activity had no influence on the relationship between DC step and average firing rate. Analysis of the influence of random GABA$_A$ activity on CV$_{ISI}$ at these 3 different E$_{GABA}$ indicated that while the level of GABA$_A$ activity had a major influence on CV$_{ISI}$ at E$_{GABA}$ = −70 or 0 mV, it had little effect on CV$_{ISI}$ at E$_{GABA}$ = −35 mV.

Thus, by regulating their GABA$_A$ receptor reversal potential, i.e. their intracellular chloride concentration [22,25], neurones retain control of how spontaneous GABAergic activity may increases or decrease excitability but also to which level the temporal fidelity of their discharge will be deteriorated.

Discussion

Ongoing background activity has been shown to have an important impact on neuronal dynamics. Changes in the level of
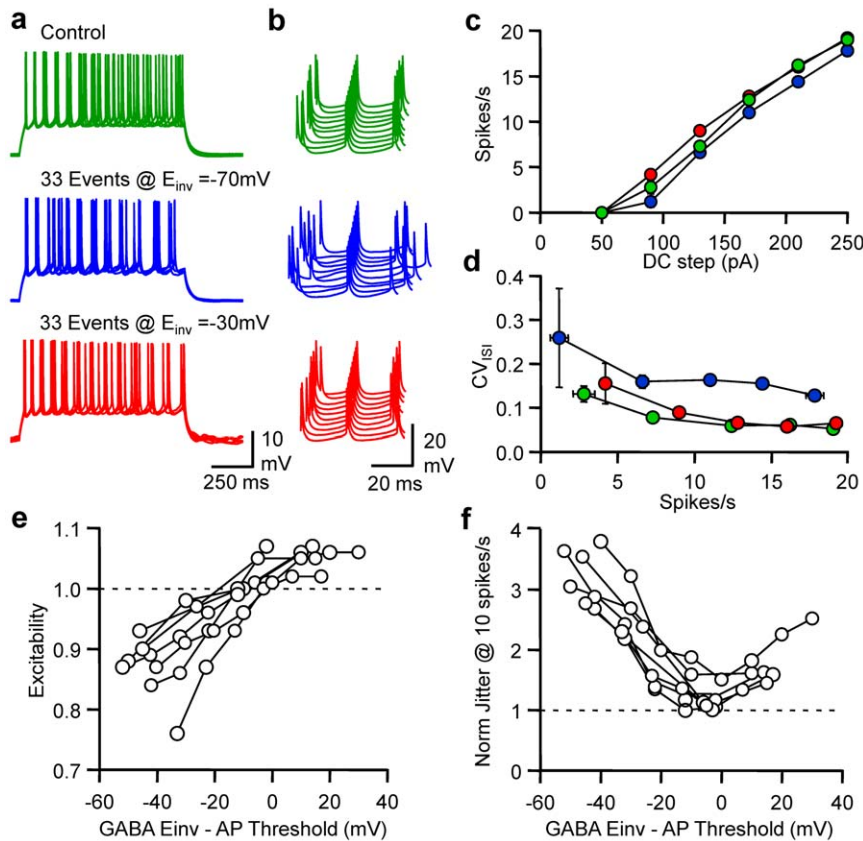
Figure 6. Reversal potential-dependent tuning of pyramidal cell excitability and discharge fidelity. a, Superimposed (5) Vm fluctuations of a whole-cell L2/3 pyramidal neurone in response to a DC step (1 s, 170 pA) in control conditions (green), when 33 randomly occurring GABA$_A$ events/s were dynamically injected at $E_{GABA} = -70$ mV (blue) or -30 mV (red). Same cell and colour code for b, c and d. b, Waterfall view of Vm when the 5th spike was set as the time reference. c, Mean firing rate vs DC step. d, CV$_{ISI}$ vs firing rate. e, Normalised changes in excitability observed when neurons received 33 randomly occurring GABA$_A$ dynamic currents/s at various differences between E_{GABA} and the calculated threshold for AP in each individual cell (n = 9). f, Normalised changes in spike jitter observed for a firing rate of 10 spikes/s. Same conditions as in e.
doi:10.1371/journal.pone.0022322.g006

background inhibition alter the electrical compactness and modify the integrative properties [13,26], modulate the gain [27] and thus can dynamically set the range of the input/output function of neurones [15–17]. Here I have emphasized the fact that GABAergic activity not only affects the excitability of pyramidal cells, but also alters spike timing in proportions that can be significantly higher, according to its temporal organisation and E_{GABA}.

## Variations in background GABAergic activity

Ongoing subthreshold activity of neocortical neurones is subject to important changes. In the anaesthetised animal, alternating states of low or intense activity can be observed: the down-states during which little or no synaptic background activity is visible and the up-states when the cells are continuously bombarded by spontaneous activity [7,8,26]. The pattern of GABAergic activity that is received by these cells is determined by the number, the variety and activity of presynaptic interneurones [28]. The complexity of the GABAergic system is enhanced by the fact that GABAergic synapses, according to their location, exhibit specific electrophysiological features [29–32]. Additionally, the level of spontaneous GABAergic activity is subject to prominent changes during development [33], short [34,35] or long-term plasticity [36–43] and can be altered in different pathologies [44–47].

In the absence of synaptic activity, the spike generating mechanism shows a certain level of reliability and precision [18]

that can be noticeably reduced by the spontaneous occurrence of few GABA$_A$ synaptic events. Experiments performed *in vitro* with endogenous GABAergic activity or computer-modelled background activity injected to the cell by the means of a dynamic-clamp amplifier could be very well predicted with a RT-LIF model. Therefore, while taking into account the fact that the experiments presented here represent only a very limited range of presynaptic activities when compared to what has been reported *in vivo* during up-states [8], the RT-LIF model appears to be, for this range level of activity, sufficiently complex to capture the essential features of the impact of GABA$_A$ activity on excitability and spike-timing.

Beyond their molecular heterogeneity, GABA$_A$ receptors can be activated following two different modes, phasic or tonic release. Phasic activation of GABA$_A$ receptors relies on synchronous opening of clustered synaptic receptors, while tonic activation results from the activation of extra synaptic receptors [21]. Results obtained in this study show that tonic and phasic inhibition modify to the same extent the input/output relationship, when a repetitive discharge was induced by step excitation. Thus, the average input/output relationship appears to be dependent neither on the timing nor the shape of the spontaneous conductance transients but rather on the average conductance over time (Fig. 4). In contrast, major differences between the mode of activation of GABA$_A$ receptors and the fidelity of spike timing were observed. Indeed the increase in variability was dependent on the average GABA$_A$
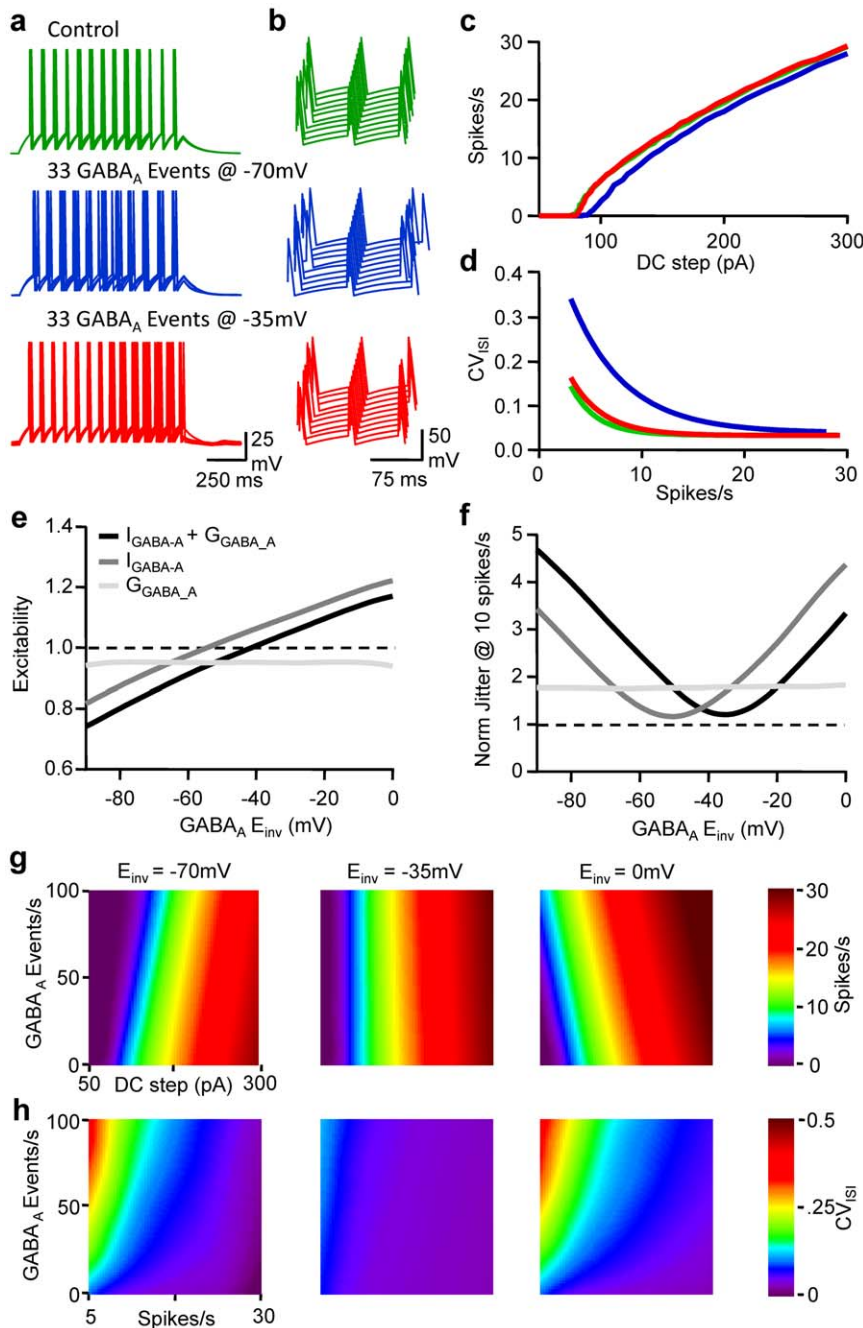
Figure 7. Frequency and reversal potential-dependent tuning of pyramidal cell excitability and discharge fidelity. a, Superimposed (5) Vm fluctuations of the LIF model in response to a DC step (1 s, 160 pA) in control conditions (green), when the LIF model received 33 randomly occurring $GABA_A$ events/s at $E_{GABA} = -70$ mV (blue) or -35 mV (red). Same colour code for b, c and d. b, Waterfall view of Vm when the 5th spike was set as the time reference. c, Mean firing rate *vs* DC step. d, CV_{ISI} *vs* firing rate. e, Normalised changes in excitability observed when LIF model received 33 randomly occurring $GABA_A$ events/s at various E_{GABA} in control conditions (black), when GABA activity induced only transient changes in I_{GABA-A} (gray) or when GABA activity induced only transient changes in R_{in} (light gray). f, Normalised changes in spike jitter observed for a rate of 10 spikes/s. Same conditions as in e. g, From left to right firing rate displayed on a pseudocolor scale *vs* DC step and E_{GABA} when the LIF model received 33 randomly occurring $GABA_A$ events/s in control conditions (left), when $GABA_A$ activity induced only transient changes in I_{GABA-A} (middle) or when GABA activity induced only transient changes in R_{in} (right). h, CV_{ISI} displayed on a pseudocolor scale *vs* firing rate and E_{GABA}. Same conditions as in g.
doi:10.1371/journal.pone.0022322.g007

conductance; it appeared first that transient changes in inhibitory conductance were more prone to disorganize firing, and second that random trains were more potent than fixed patterns of experimentally derived synaptic conductance waveforms.

In fact, from a control condition where the action potential delay is dependent on the AHP amplitude, the membrane time constant and the voltage threshold for action potential, transient inhibitory conductances delay Vm from reaching action potential threshold and thus induce both an increase in ISI mean and variability, such that the temporal structure of neuronal discharge is rapidly lost. If now the timing of transient inhibitory conductances remains invariable, the probability of firing an action

potential is not uniform but varies according to the pattern of inhibitory conductance (Fig. 5). As demonstrated by Mainen and Sejnowski [18], when a DC pattern is invariably replayed, the reliability of the firing pattern increases as a function of the fluctuation amplitude. Tiesinga and Toups [48] later showed that an invariable fluctuating DC pattern uncovers, after a statistical sorting of the different trials, a series of precise spike patterns with different spike times and eventually a different number of spikes [49]. Thus, the variance of inputs uncovers different spike patterns and maintains a high probability of spike timing in narrow windows all along the discharge, but increases the variability of the ISI. In contrast tonic inhibition, whatever the analysis method employed (CV_{ISI} or firing probability over time) barely deteriorates spike timing. Pouille and Scanziani [19] have demonstrated that feed forward inhibition curtailed EPSPs and improved EPSP-spike timing *in vitro*. In some specific GABAergic interneurones, because autaptic transmission offers a tight temporal link between the spike and GABAergic conductance, the reliability of spike timing is greatly improved by the activation of autaptic $GABA_A$ receptors [20]. Despite the fact that in these two latter examples, where a subpopulation of GABAergic synapses is activated sequentially after some excitatory synaptic inputs or neuronal discharge, the temporal structure of most of the GABAergic activity is often uncorrelated to pre or postsynaptic activity. From the results described here, reducing the fidelity of discharge by adding tonic or phasic inhibition may at first sight appear contradictory with previously published results. However one has to take into account the fact that here $GABA_A$ activity was not time-locked to patterns of EPSPs and also that fidelity was measured and compared for similar rates of spike discharge. It demonstrates that, once neurones trigger action potentials at a sustained rate, the consequences of a given amount of GABA, whatever its mode of release i.e. phasic random *vs* phasic invariable *vs* tonic, is quantitatively the same on excitability, but appears to be different on spike timing. While tonic activation of $GABA_A$ receptors contributes to the modulation of excitability and thus may have a key role in epileptogenicity [50], its ability to disorganise firing discharge seems limited. In conclusion, excitability and spike timing modulation by $GABA_A$ receptors are not strictly related, but rely on the mode of GABA release and the eventual temporal correlation between the activation of $GABA_A$ receptors, the excitatory inputs and action potential firing in case of repetitive discharge.

Variations in $GABA_A$ reversal potential

$GABA_A$ receptors are permeable to chloride and bicarbonate ions [51]. As bicarbonate ions are much less permeant than chloride, and because the chloride equilibrium potential is usually more negative than the resting membrane potential, activation of $GABA_A$ receptors typically results in a hyperpolarising inhibitory postsynaptic potential. Nevertheless, the chloride gradient is developmentally regulated and subject to plasticity [25]. A large range of $GABA_A$ reversal potentials has been reported in the past twenty years [52]. Evoked GABAergic activity was shown to affect the timing of spikes evoked by membrane potential oscillations, according to the phase at which $GABA_A$ receptors were activated and E_{GABA} [53]. According to development, the neural situation, depolarised E_{GABA} may be relevant and required for proper network activity, though consideration has to be given that this will modify the temporal organisation of the postsynaptic discharge and the stability of network oscillations [53].

From the present study it appears that intracellular chloride homeostasis has a very important role in defining the changes in excitability and fidelity induced by a given rate of presynaptic GABA release. Spike timing jitter is closely proportional to the absolute difference between the threshold for action potential and E_{GABA}. From this study it appears that, for a given rate of GABAergic activity, both the changes in membrane resistance and the currents associated with $GABA_A$ conductance affect excitability and spike timing. Excitability and spike time jitter are proportional to $GABA_A$ conductance. Thus, in order to compensate for changes in excitability induced by $GABA_A$ activity and the associated reduction in membrane resistance, E_{GABA} must be higher than the threshold for action potential generation. In the case of no change in membrane resistance associated with $GABA_A$ conductance, as is the case in the dynamic-clamp experiments, E_{GABA} appeared lower than the threshold for action potential. Since $GABA_A$ currents tune excitability and spike timing, the reversal potential where $GABA_A$ activity has the minimal impact appears to be the potential at which the $GABA_A$ currents are on average equal to zero. Thus, the electrophysiological characteristics of a given neuron may be associated with a specific E_{GABA} such that the changes in excitability and reduction in spike timing reliability by GABAergic activity may be alleviated.

Spike-timing and network activity

Neuronal coding of sensory information relies on the mean rate of action potential discharge but also the relative timing between action potentials. Stimulus-dependent changes in spike synchronization have been observed in various cortical areas, and it has been suggested that synchronization of spikes within a precise millisecond range could serve as an efficient mechanism to group neurons into cell assemblies responding to specific stimuli [54,55]. During stimulus processing the recruitment of excitatory neurons and their connections are often the primary requisites for neuronal computation. GABAergic neurones contribute to synchronization. In invertebrates, $GABA_A$ receptors were shown to be of critical importance as their blockade abolished oscillatory synchronization but not the individual responsiveness of projection neurones [56]. The presence of feed-forward inhibition or autaptic synapses in various areas of the central nervous system may be critical to maintain spike timing and synchrony [19,20,53]. Nevertheless, most of the phasic GABAergic activity appears not to be correlated with sensory stimuli [26], tonic inhibition is present in different brain areas [21] and asynchronous release of GABA is observed in CCK-interneurones in the hippocampus [57–59]. Thus, synaptic and extra-synaptic $GABA_A$ receptors can be activated in various modes, which share common characteristics but also particular features that may have computational significance for the regulation of network activity.

In conclusion, I have emphasized in this study the fact that, in addition to the well-documented modulation of neuronal excitability, spontaneous GABAergic activity has a major detrimental impact on spike timing reliability. A future challenge is to understand how variability in spike timing contributes to neuronal processing in the brain, in this context the impact of GABA release and chloride homeostasis in deteriorating spike timing should not be neglected.

Materials and Methods

Ethics Statement

All rats were maintained on a 12 h light/dark cycle with food and water provided ad libitum. The research involving animals has been approved by the Direction Départementale des Services Vétérinaires – Préfecture des Bouches du Rhône, France (permit number C13-055-8), and the Institut Jean-Roche Animal Care Supervisor (M. Mekahouche, D.V.M Ph.D, permit number 13-122).

All experiments were carried out according to the European and Institutional guidelines for the care and use of laboratory animals (Council Directive 86/609/EEC and French National Research Council).

Cortical slice preparation and electrophysiological recordings

Transverse cortical slices (350–400 µm thick) were obtained from 13- to 20-day old Wistar rats as previously described [60]. Experiments were performed at 32°C in ACSF containing the following (in mM): NaCl 125, NaHCO3 26, CaCl2 3, KCl 2.5, MgCl2 2, NaH2PO4 0.8, D-glucose 10, kynurenate (2 mM); and saturated with 95% O_2 and 5% CO_2. L2/3 pyramidal cells (recorded between 300 and 800 µm from the pia) were visualised using an Olympus BX-51 WI microscope equipped with differential interference contrast optics under infrared illumination and a water immersion lens (X60, 0.9 NA, Olympus). Unless otherwise stated, electrophysiological recordings were performed in whole-cell configuration with a Multiclamp 700B amplifier (Axon Instruments), filtered at 5 kHz and digitized at 20 kHz via a PCI-6220 National Instrument interface controlled by IgorPro (Wavemetrics) and/or Digidata 1322A interface controlled by PClamp software (Axon Instruments). Patch pipettes had a resistance of 3–6 MΩ when filled with a solution containing (in mM): K-gluconate 120, KCl 20, HEPES 10, EGTA 0.5, Na2ATP 2, NaGTP 0.3, and MgCl2 2, pH 7.4. Cells were recorded if the series resistance, measured throughout experiments, remained stable and <20 MOhm. In a subset of experiments (Fig. 1, Fig. S1c,d), perforated patch-clamp recordings were performed. Gramicidin (100 µg/ml) was added to the intracellular solution. For this recording configuration the tip of the pipette was back-filled with the solution containing no gramicidin to allow a good cell-attached configuration prior to perforation by gramicidin diffusion at the tip of the pipette. Alexa 488 or 568 (Molecular Probes) were added to the intracellular solution in order to confirm the pyramidal cell morphology in some whole-cell recordings. Fluorescence excitation was performed using a PolyV monochromator (Till photonics). Fluorescence imaging was performed with a CCD Camera (CoolSnap HQ2). Both excitation patterns and fluorescence acquisition were controlled by Metavue (Molecular Devices) and IgorPro (Wavemetrics) software. Isoguvacine (0.5 mM) was pressure ejected using a pico-Spritzer (TooheySpritzer). Typical pressure and time ejection were 7PSI and 30 ms respectively. Alexa 588 (Molecular Probes) was added to the isoguvacine solution in order to visualise its diffusion when ejected. During the course of the perforated patch-clamp recordings, E_{GABA} was estimated from the polarity of isoguvacine responses at different holding membrane potential. This protocol inform me, together with alexa 488 dye imaging that perforated patch did not evolve into whole cell mode during the course of the experiment, Electrophysiological recordings were stopped if a sudden change in E_{GABA} or fluorescence of the soma was observed.

Picrotoxin (100 mM) was prepared in ethanol and stored at −80°C. Kynurenate (200 mM) was prepared in distilled water and stored at −20°C (respectively). Stocks solutions were thawed and diluted into the extracellular solution before use.

Stimuli

Voltage or DC steps, GABA_A synaptic conductances and reversal potentials were constructed, according to experimental needs with Igor Pro software (Wavemetrics), and converted to analog signals via a PCI-6723 National Instrument interface. GABA_A like currents were simulated with a dynamic-clamp amplifier (SM1, Cambridge Conductance), using for inputs the conductance profile, the reversal potential and the membrane potential of the recorded cell. The calculated current was summed to the DC step and injected into the recorded cell.

Neuronal modelling

GABAergic synaptic events were modelled as a conductance with a dual exponential time course of the form (1-exp(-t/tau_rise).exp(-t/tau_decay). Spontaneous activity was created by convolution of the GABAergic event template with the Poisson train occurrence of spontaneous events. The conductance instruction was then either converted to an analog signal to instruct the dynamic clamp amplifier or injected to the computational model. The latter was based on a leaky integrate and fire model (LIF) with random threshold [23,24] unless otherwise stated: $C_m.dV_i/dt = Sigma_i.g_i.(V_O-V_i)+Sigma_i.I$ with $C_m = 400$ pF; $V_o = -65$ mV. When V_i reaches a threshold theta, a spike is generated and the membrane potential resets to V_o. Resting membrane resistance was set at 200 MOhm. GABAergic synaptic events, affecting both g_i and I were sometimes included, according to the equation $I_{GABA} = g_{GABA}.(V_m-E_{GABA})$. E_{GABA} was set at −70 mV unless otherwise stated. All modelling was performed with Igor Pro Software.

Analysis

Spontaneous synaptic activity was analyzed with the help of Minianalysis (Synaptosoft, Decatur, GA, USA). Spike analysis was performed with Igor Pro (Wavemetrics, Lake Oswego, OR, USA), Neuromatic functions (Jason Rothman, http://www.neuromatic.thinkrandom.com) were used in addition to homemade functions. 3D graphs were drawn under Origin Pro 8.0 (Origin Lab, Northampton, MA, USA) by smoothing average data with a thin plate spline function.

Spike Threshold was detected when dV/dt exceeded 10 mV/ms. Measurements of CV_{ISI} were performed by averaging CV for each sequential interval along the discharge starting from the 2nd spike. With this method, the reproducibility of the full discharge for one trial to another could be evaluated, independently of spike-frequency adaptation that was observed experimentally.

Measurement of spike time jitter @ 10 spikes/s was performed by interpolating the CV_{ISI} vs average spike discharge with either the best linear or exponential fit.

Plots of firing probability (fig. 5) were obtained by convolving the times of spike generation with a Gaussian function with standard deviation equal to the duration of the sweep, divided by the mean number of spikes [61]. Statistical comparisons were made using ANOVA paired tests. Differences were considered significant when P<0.05. Data are reported as mean ± s.e.m.

Supporting Information

Figure S1   Characteristics of spontaneous GABA_A events received by L2/3 pyramidal cells. a, Spontaneous occurrence of GABAergic current transients recorded in a L2/3 pyramidal cell ($V_{hold} = -70$ mV). Their frequency was on average 3.8±1.0 events/s (range 0.9–13.1 events/s, n = 15). b, Average GABA_A current transients (from n = 66 events) received by the cell shown in a. For all cells tested GABA_A current transients were displayed a fast 10–90% rise time (1.5±0.2 ms, range 0.6–3.7 ms, n = 15); the conductance at the peak of current was 343±28 nS (range 146–508 nS, n = 15); their tail was best fitted with a monoexponential decay (time constant 14.7±1.1 ms, range 7.2–21.4, n = 15). c, superimposed currents in response to a brief (15 ms) perisomatic pressure ejection of GABA_A agonist isoguvacine at 4 different V_{hold} (−88,−78,−68,−58 mv) during a gramicidin perforated voltage-clamp recording. d, GABA_A current

measured at the peak of isoguvacine response vs V$_{hold}$. Same cell as in c. E$_{GABA}$ was on average -69 ± 4 mV (range -82–-57 mV; n = 5).
(TIF)

Figure S2 Leaky Integrate and Fire Model with Random Action Potential Threshold. a, Electronic Design of the Leaky Integrate and Fire Model. It is based on an RC circuit with a condition: if Vm crosses the Threshold Θ, an action potential waveform lasting 10 ms, that peaks at +30 mV and resets at -60 mV, is added. b, Θ can be either invariable (green line) or random when adding a Gaussian noise to Θ (red SDV = 1 mV). c, Superimposed (5) Vm fluctuations of the LIF model in response to a DC step (1 s, 160 pA) and Waterfall view of the Vm in order to show the jitter of the previous and following spikes when the 5th spike was set as a the time reference in control (green; SDV Θ = 0 mV), or when SDV Θ = 1 mV (red). d,. Mean firing rate vs DC step. Same colour code as in c. e, CV$_{ISI}$ vs firing rate when SDV Θ = 1 mV. CV remains null if SDV Θ = 0 mV.
(TIF)

Figure S3 Contributions of GABA$_A$ current and GABA$_A$ shunt to the frequency-dependent tuning in Excitability and Fidelity. a, From upper to lower, a G$_{GABA-A}$ pattern of 33 events/s, Vm, sum of the DC step (135 pA)+I$_{GABA-A}$ and membrane input resistance (R$_{in}$) fluctuations in the LIF model when E$_{GABA}$ was set at -70 mV. b, Same conditions as in a but R$_{in}$ remained constant despite transient changes in G$_{GABA-A}$. c, Same conditions as in a but I$_{GABA-A}$ remained null during the simulation despite transient changes in G$_{GABA-A}$. d, Mean firing rate displayed on a pseudocolor scale vs DC step and the rate of randomly occurring GABA$_A$ activity in control conditions (left), when GABA$_A$ activity induces only transient changes in GABA$_A$ currents (middle) and when GABA$_A$ activity induces only transient changes in R$_{in}$ (right). e, CV$_{ISI}$ displayed on a pseudocolor scale vs firing and GABA$_A$ activity rate. Same conditions as in d.
(TIF)

Figure S4 Amplitude- and Frequency-dependent tuning of pyramidal cell discharge fidelity by randomly occurring GABA$_A$ conductance transients. a, From upper to lower, a G$_{GABA-A}$ pattern of 33 events/s, Vm, sum of the DC step (135 pA)+I$_{GABA-A}$ and membrane input resistance (R$_{in}$) fluctuations in the LIF model when E$_{GABA}$ was set at -70 mV. Peak GABA$_A$ conductance was set at 0.5 nS. b, Same conditions as in a but peak GABA$_A$ conductance was set at 1 nS. c, Same conditions as in a but peak GABA$_A$ conductance was set at 2 nS. d, Mean

firing rate displayed on a pseudocolor scale vs DC step and the rate of randomly occurring GABA$_A$ activity when Peak GABA$_A$ conductance was set at 0.5 nS (left), 1 nS (middle) and 2 nS (right). e, CV$_{ISI}$ displayed on a pseudocolor scale vs firing and GABA$_A$ activity rate. Same conditions as in d.
(TIF)

Figure S5 The kinetics of randomly occurring normalised GABA$_A$ conductance transients do not affect the frequency-dependent tuning of Excitability and Fidelity. a, From upper to lower, a G$_{GABA-A}$ pattern of 33 events/s, Vm, sum of the DC step (135 pA)+I$_{GABA-A}$ and membrane input resistance (R$_{in}$) fluctuations in the LIF model when E$_{GABA}$ was set at -70 mV. Peak GABA$_A$ conductance was set at 2.005 nS, and GABA$_A$ conductance transients had fast kinetics (Tau$_{rise}$ = 0.5 ms; Tau$_{decay}$ = 5 ms). b, Same conditions and GABA$_A$ charge as in a but GABA$_A$ conductance transients had medium kinetics (Peak GABA$_A$ conductance = 1 nS; Tau$_{rise}$ = 1 ms; Tau$_{decay}$ = 10 ms). c, Same conditions as in a but GABA$_A$ conductance transients had slow kinetics (Peak GABA$_A$ conductance = 0.2268 nS; Tau$_{rise}$ = 10 ms; Tau$_{decay}$ = 30 ms). d, Mean firing rate displayed on a pseudocolor scale vs DC step and the rate of randomly occurring GABA$_A$ activity when GABA$_A$ conductance transients had parameters depicted in a (fast kinetics, left), when GABA$_A$ conductance transients had parameters depicted in b (medium kinetics, middle) and when GABA$_A$ conductance transients had parameters depicted in c (slow kinetics, right). e, CV$_{ISI}$ displayed on a pseudocolor scale vs firing and GABA$_A$ activity rate. Same conditions as in d.
(TIF)

Author Contributions

Conceived and designed the experiments: OC. Performed the experiments: OC. Analyzed the data: OC. Contributed reagents/materials/analysis tools: OC. Wrote the paper: OC.

References

1. Schneidman E, Freedman B, Segev I (1998) Ion channel stochasticity may be critical in determining the reliability and precision of spike timing. Neural Comput 10: 1679–1703.
2. Jacobson GA, Diba K, Yaron-Jakoubovitch A, Oz Y, Koch C, et al. (2005) Subthreshold voltage noise of rat neocortical pyramidal neurones. J Physiol 564: 145–160.
3. Arieli A, Sterkin A, Grinvald A, Aertsen A (1996) Dynamics of ongoing activity: Explanation of the large variability in evoked cortical responses. Science 273: 1868–1871.
4. Azouz R, Gray CM (1999) Cellular mechanisms contributing to response variability of cortical neurons in vivo. J Neurosci 19: 2209–2223.
5. Tsodyks M, Kenet T, Grinvald A, Arieli A (1999) Linking spontaneous activity of single cortical neurons and the underlying functional architecture. Science 286: 1943–1946.
6. Boly M, Balteau E, Schnakers C, Degueldre C, Moonen G, et al. (2007) Baseline brain activity fluctuations predict somatosensory perception in humans. Proc Natl Acad Sci U S A 104: 12187–12192.
7. Brecht M, Roth A, Sakmann B (2003) Dynamic receptive fields of reconstructed pyramidal cells in layers 3 and 2 of rat somatosensory barrel cortex. J Physiol 553: 243–265.
8. Destexhe A, Rudolph M, Pare D (2003) The high-conductance state of neocortical neurons in vivo. Nat Rev Neurosci 4: 739–751.
9. Gulledge AT, Stuart GJ (2003) Action potential initiation and propagation in layer 5 pyramidal neurons of the rat prefrontal cortex: absence of dopamine modulation. J Neurosci 23: 11363–11372.
10. Glickfeld LL, Roberts JD, Somogyi P, Scanziani M (2009) Interneurons hyperpolarize pyramidal cells along their entire somatodendritic axis. Nat Neurosci 12: 21–23.
11. Rheims S, Minlebaev M, Ivanov A, Represa A, Khazipov R, et al. (2008) Excitatory GABA in rodent developing neocortex in vitro. J Neurophysiol 100: 609–619.
12. Pare D, Lang EJ, Destexhe A (1998) Inhibitory control of somatodendritic interactions underlying action potentials in neocortical pyramidal neurons in vivo: an intracellular and computational study. Neuroscience 84: 377–402.
13. Destexhe A, Pare D (1999) Impact of network activity on the integrative properties of neocortical pyramidal neurons in vivo. J Neurophysiol 81: 1531–1547.
14. Wiesenfeld K, Moss F (1995) Stochastic resonance and the benefits of noise: from ice ages to crayfish and SQUIDs. Nature 373: 33–36.

15. Wolfart J, Debay D, Le MG, Destexhe A, Bal T (2005) Synaptic background activity controls spike transfer from thalamus to cortex. Nat Neurosci 8: 1760–1767.

16. Aradi I, Santhakumar V, Chen K, Soltesz I (2002) Postsynaptic effects of GABAergic synaptic diversity: regulation of neuronal excitability by changes in IPSC variance. Neuropharmacology 43: 511–522.

17. Aradi I, Santhakumar V, Soltesz I (2004) Impact of heterogeneous perisomatic IPSC populations on pyramidal cell firing rates. J Neurophysiol 91: 2849–2858.

18. Mainen ZF, Sejnowski TJ (1995) Reliability of spike timing in neocortical neurons. Science 268: 1503–1506.

19. Pouille F, Scanziani M (2001) Enforcement of temporal fidelity in pyramidal cells by somatic feed-forward inhibition. Science 293: 1159–1163.

20. Bacci A, Huguenard JR (2006) Enhancement of spike-timing precision by autaptic transmission in neocortical inhibitory interneurons. Neuron 49: 119–130.

21. Farrant M, Nusser Z (2005) Variations on an inhibitory theme: phasic and tonic activation of GABA(A) receptors. Nat Rev Neurosci 6: 215–229.

22. Kahle KT, Staley KJ, Nahed BV, Gamba G, Hebert SC, et al. (2008) Roles of the cation-chloride cotransporters in neurological disease. Nat Clin Pract Neurol 4: 490–503.

23. Holden AV (1976) Models of stochastic activity of neurones. New York: Springer-Verlag.

24. Manwani A, Steinmetz PN, Koch C (2002) The impact of spike timing variability on the signal-encoding performance of neural spiking models. Neural Comput 14: 347–367.

25. Payne JA, Rivera C, Voipio J, Kaila K (2003) Cation-chloride co-transporters in neuronal communication, development and trauma. Trends Neurosci 26: 199–206.

26. Pare D, Shink E, Gaudreau H, Destexhe A, Lang EJ (1998) Impact of spontaneous synaptic activity on the resting properties of cat neocortical pyramidal neurons In vivo. J Neurophysiol 79: 1450–1460.

27. Chance FS, Abbott LF, Reyes AD (2002) Gain modulation from background synaptic input. Neuron 35: 773–782.

28. Ascoli GA, Alonso-Nanclares L, Anderson SA, Barrionuevo G, Benavides-Piccione R, et al. (2008) Petilla terminology: nomenclature of features of GABAergic interneurons of the cerebral cortex. Nat Rev Neurosci 9: 557–568.

29. Miles R, Toth K, Gulyás AI, Hájos N, Freund TF (1996) Differences between somatic and dendritic inhibition in the hippocampus. Neuron 16: 815–823.

30. Pearce RA (1993) Physiological evidence for two distinct GABAA responses in rat hippocampus. Neuron 10: 189–200.

31. Sceniak MP, MacIver MB (2008) Slow GABA(A) mediated synaptic transmission in rat visual cortex. BMC Neurosci 9: 8.

32. Jedlicka P, Deller T, Gutkin BS, Backus KH (2010) Activity-dependent intracellular chloride accumulation and diffusion controls GABA(A) receptor-mediated synaptic transmission. Hippocampus.

33. Colin-Le Brun I, Ferrand N, Caillard O, Tosetti P, Ben Ari Y, et al. (2004) Spontaneous synaptic activity is required for the formation of functional GABAergic synapses in the developing rat hippocampus. J Physiol 559: 129–139.

34. Llano I, Leresche N, Marty A (1991) Calcium entry increases the sensitivity of cerebellar Purkinje cells to applied GABA and decreases inhibitory synaptic currents. Neuron 6: 565–574.

35. Pitler TA, Alger BE (1992) Postsynaptic spike firing reduces synaptic GABAA responses in hippocampal pyramidal cells. J Neurosci 12: 4122–4132.

36. McLean HA, Caillard O, Khazipov R, Ben-Ari Y, Gaïarsa J-L (1996) Spontaneous release of GABA activates GABAB receptors and controls network activity in the neonatal rat hippocampus. J Neurophysiol 76: 1036–1046.

37. Caillard O, Ben Ari Y, Gaïarsa J-L (1999) Mechanisms of induction and expression of long-term depression at GABAergic synapses in the neonatal rat hippocampus. J Neurosci 19: 7568–7577.

38. Hashimoto T, Ishii T, Ohmori H (1996) Release of Ca2+ is the crucial step for the potentiation of IPSCs in the cultured cerebellar Purkinje cells of the rat. J Physiol 497(Pt 3): 611–627.

39. Rutherford LC, DeWan A, Lauer HM, Turrigiano GG (1997) Brain-derived neurotrophic factor mediates the activity-dependent regulation of inhibition in neocortical cultures. J Neurosci 17: 4527–4535.

40. Kang J, Jiang L, Goldman SA, Nedergaard M (1998) Astrocyte-mediated potentiation of inhibitory synaptic transmission. Nat Neurosci 1: 683–692.

41. Caillard O, Ben Ari Y, Gaïarsa J-L (1999) Long-term potentiation of GABAergic synaptic transmission in neonatal rat hippocampus. J Physiol (Lond) 518: 109–119.

42. Galante M, Nistri A, Ballerini L (2000) Opposite changes in synaptic activity of organotypic rat spinal cord cultures after chronic block of AMPA/kainate or glycine and GABAA receptors. J Physiol 523 Pt 3: 639–651.

43. Ouardouz M, Sastry BR (2000) Mechanisms underlying LTP of inhibitory synaptic transmission in the deep cerebellar nuclei. J Neurophysiol 84: 1414–1421.

44. Hirsch JC, Agassandian C, Merchan-Perez A, Ben-Ari Y, DeFelipe J, et al. (1999) Deficit of quantal release of GABA in experimental models of temporal lobe epilepsy. Nat Neurosci 2: 499–500.

45. Kobayashi M, Wen X, Buckmaster PS (2003) Reduced inhibition and increased output of layer II neurons in the medial entorhinal cortex in a model of temporal lobe epilepsy. J Neurosci 23: 8471–8479.

46. Kobayashi M, Buckmaster PS (2003) Reduced inhibition of dentate granule cells in a model of temporal lobe epilepsy. J Neurosci 23: 2440–2452.

47. El-Hassar L, Milh M, Wendling F, Ferrand N, Esclapez M, et al. (2007) Cell domain-dependent changes in the glutamatergic and GABAergic drives during epileptogenesis in the rat CA1 region. J Physiol 578: 193–211.

48. Tiesinga PH, Toups JV (2005) The possible role of spike patterns in cortical information processing. J Comput Neurosci 18: 275–286.

49. Tiesinga P, Fellous JM, Sejnowski TJ (2008) Regulation of spike timing in visual cortical circuits. Nat Rev Neurosci 9: 97–107.

50. Cope DW, Di GG, Fyson SJ, Orban G, Errington AC, et al. (2009) Enhanced tonic GABAA inhibition in typical absence epilepsy. Nat Med 15: 1392–1398.

51. Kaila K (1994) Ionic basis of GABAA receptor channel function in the nervous sytem. Prog Neurobiol 42: 489–537.

52. Marty A, Llano I (2005) Excitatory effects of GABA in established brain networks. Trends Neurosci 28: 284–289.

53. Stiefel KM, Wespatat V, Gutkin B, Tennigkeit F, Singer W (2005) Phase dependent sign changes of GABAergic synaptic input explored in-silicio and in-vitro. J Comput Neurosci 19: 71–85.

54. Kreiter AK, Singer W (1996) Stimulus-dependent synchronization of neuronal responses in the visual cortex of the awake macaque monkey. J Neurosci 16: 2381–2396.

55. deCharms RC, Merzenich MM (1996) Primary cortical representation of sounds by the coordination of action-potential timing. Nature 381: 610–613.

56. MacLeod K, Laurent G (1996) Distinct mechanisms for synchronization and temporal patterning of odor-encoding neural assemblies. Science 274: 976–979.

57. Hefft S, Jonas P (2005) Asynchronous GABA release generates long-lasting inhibition at a hippocampal interneuron-principal neuron synapse. Nat Neurosci 8: 1319–1328.

58. Ali AB, Todorova M (2010) Asynchronous release of GABA via tonic cannabinoid receptor activation at identified interneuron synapses in rat CA1. Eur J Neurosci 31: 1196–1207.

59. Daw MI, Tricoire L, Erdelyi F, Szabo G, Mcbain CJ (2009) Asynchronous transmitter release from cholecystokinin-containing inhibitory interneurons is widespread and target-cell independent. J Neurosci 29: 11112–11122.

60. Debanne D, Boudkkazi S, Campanac E, Cudmore RH, Giraud P, et al. (2008) Paired-recordings from synaptically coupled cortical and hippocampal neurons in acute and cultured brain slices. Nat Protoc 3: 1559–1568.

61. Axmacher N, Miles R (2004) Intrinsic cellular currents and the temporal precision of EPSP-action potential coupling in CA1 pyramidal cells. J Physiol 555: 713–725.